Sequence Generator Network for Neuromechanical Control of Rat Hindlimbs

Clayton B. Jackson[1(✉)], William R. P. Nourse[2], and Roger D. Quinn[1]

[1] Department of Mechanical and Aerospace Engineering, Case Western Reserve University, Cleveland, OH 44106-7222, USA
clayton.jackson@case.edu

[2] Department of Electrical, Computer, and Systems Engineering, Case Western Reserve University, Cleveland, OH 44106-7222, USA

Abstract. Mammalian locomotion is a complex behavior arising from interaction between neural and biomechanical systems, driven by rhythmic activity originating in the spinal cord. Although it has been extensively studied, the structure of the circuits that produce this behavior remains unknown. One approach to modeling the rhythmic activity is with half-center models, in which there are alternating periods of flexion and extension to coordinate muscle activity. While this approach is sufficient for simple antagonistic muscle pairs, it can be difficult to expand the controller for more complex models with muscle synergies. This work introduces a method of modeling the activity in the spinal cord with a population of neurons exhibiting a continuous cycle of activity, rather than the push-pull of half-centers. To evaluate the effectiveness of this neural model for locomotive behavior, we integrate it with a biomechanical simulation to control the muscle activity in a pair of rat hindlimbs. With this controller, a pair of simulated rat hindlimbs is able to walk on the ground with joint trajectories exhibiting similar features to the animal during locomotion. This model of the spinal cord activity shows promising results on a simple model and demonstrates the ability to be adapted to control more complex biomechanical models with muscle synergies.

Keywords: Pattern Generation · Neuromechanical Simulation · Mammalian Locomotion

1 Introduction

Mammalian locomotion showcases the remarkable adaptability of biological systems. From navigating rugged terrain to scaling tree branches, mammals exhibit a variety of locomotor behaviors. Central to these locomotion abilities is the

This work was supported by NSF DBI 2015317 as part of the NSF/CIHR/DFG/FRQ/UKRI-MRC Next Generation Networks for Neuroscience Program.

N. S. Szczecinski et al. (Eds.): Living Machines 2024, LNAI 14930, pp. 368–381, 2025.
https://doi.org/10.1007/978-3-031-72597-5_25

interaction between their neural control mechanisms and biomechanical systems, with the spinal cord playing a crucial role in coordinating their complex movements [10]. Central Pattern Generators (CPG's) in the spinal cord generate rhythmic behavior autonomously and, thus, are a key to vertebrate locomotion behavior [18]. While these circuits have been studied in animals (i.e. salamanders, lamprey, crabs), the structure of locomotion pattern generators remains a mystery [9,19,25,30].

A common approach to modeling the rhythmic activity in the spinal cord is using a half center model [7]. The half center model is based on the principle of escape and release, alternating between periods of flexion and extension. The half centers represent a simplified model of the spinal cord and classifies motor neurons and muscles to be either flexors or extensors. However, locomotion requires the coordination of complex muscle synergies that cannot be simplified to antagonistic pairs [15–17,36]. Other works have expanded the traditional half center model to include multiple layers of half centers to allow for more complex muscle activation, as well as the ability to control the frequency and amplitude of the motor neuron activity independently [14,29]. However, these models rely on accurate tuning of parameters and small changes to these parameters may result in significant changes in behavior. Recent studies have shown that optogenetic stimulation to the brain stem of a rat can cause a movement arrest or freezing behavior [6]. Due to the bi-stable nature of the half center models, this sort of stimulation would not result in an immediate ceasing of movement, but rather the animal would continue to move until the neural system reached an equilibrium point. The BSG model behaves similarly but features a greater number of equilibrium points, which may result in a more immediate cessation of movement, offering improved control results.

Another method of modeling the rhythmic activity in the spinal cord can be achieved by taking advantage of population dynamics. A model referred to as the Balanced Sequence Generator (BSG), has been proposed to capture the rotational dynamics observed in the spinal cord during rhythmic movement [24]. Rather than alternating periods of flexion and extention, the BSG provides a continuous cycle of neuron activity which may allow for more complex control of biomechanical models and muscle activations. The BSG is constructed using a pool of randomly connected neurons and is able to change its frequency and amplitude independently. However, the network requires principle component and sensitivity analysis in order to classify its rotational properties and determine which neurons are able to produce these changes when an additional input is applied [24]. As this network represents a low-dimensional trajectory, we can use design principles from Recurrent Neural Networks (RNNs) to design a network similar to the BSG, achieving rotational dynamics with continuous neural activity [5]. With this approach, the network is designed to meet certain criteria rather than analyzed after the fact. Models such as these have been developed, but have yet to be used for the purposes of controlling a biomechanical model [5]. The purpose of this work is to evaluate the effectiveness of such a controller which uses continuous cycles of neuron activity as a CPG for locomotion.

2 Methods

2.1 Modeling

The computational modeling in this work is done through integrating two software packages. We first create a biomechanical model of rat hindlimbs with muscles in the physics simulator Mujoco, which can then be controlled in Python [34]. The neural controller is then designed using SNS-Toolbox, a Python package developed to design and simulate Synthetic Nervous Systems (SNS) [28]. The physics and neural simulations are integrated using a traditional forward Euler method with a time step of 0.1 ms.

Biomechanical Model. The biomechanical model of rat hindlimbs was adapted from previous works which also focused on bio-inspired control schemes [14,22]. The skeleton model used was adapted from a model in OpenSim [12,23,31]. As our model only contains the hindlimbs and pelvis, constraints must be placed such that the model does not immediately fall or tip over. Previous models built in Animatlab2, a neuromechanical simulation software designed by Cofer et. al., placed additional bodies in front of and behind the hindlimbs with a fixed relationship to the pelvis [11,14]. This effectively constrained the model, preventing it from falling to the ground as well as limiting the roll and pitch angles. However, this created additional mass and frictional forces. Rather than placing these additional bodies, the same constraints were achieved in Mujoco by placing hinge and prismatic joints at the pelvis, relative to the ground, with limited ranges (see Fig. 1).

The model of the hindlimbs has also been updated to include passive compliance in the toes of the rat. It has been shown that adding passive compliance in robots can increase stability by allowing the foot to conform to the terrain and increasing the number of contact points [4,8,27]. Based on Alexander (1990), this principle can also be inferred about animals, where the pads on their feet act to reduce the force at impact and conform to the ground [3]. In previous models with rigid feet, the model walked on its toes with a single point of contact on each leg. By adding joints in the toes with stiffness and damping, we can see an increase in the number of contact points between the model and the ground, as shown in Fig. 1. The addition of these passive joints allows the model to conform to the ground and results in a more realistic and stable biomechanical model.

Our model of the rat hindlimbs uses flexor-extensor muscle pairs to control the hip, knee, and ankle joints in the sagittal plane. The muscle attachment points and maximum forces were adapted from the model presented in Deng et al. (2019) and are implemented in Mujoco using a Hill type muscle model [20]. The muscle force generated, as implemented in Mujoco, is a function of the length, velocity, and motor neuron activity [34]:

$$F_M = (F_L(L) \cdot F_v(v) \cdot A(V_{MN}) + F_P(L)) \cdot F_0 \tag{1}$$

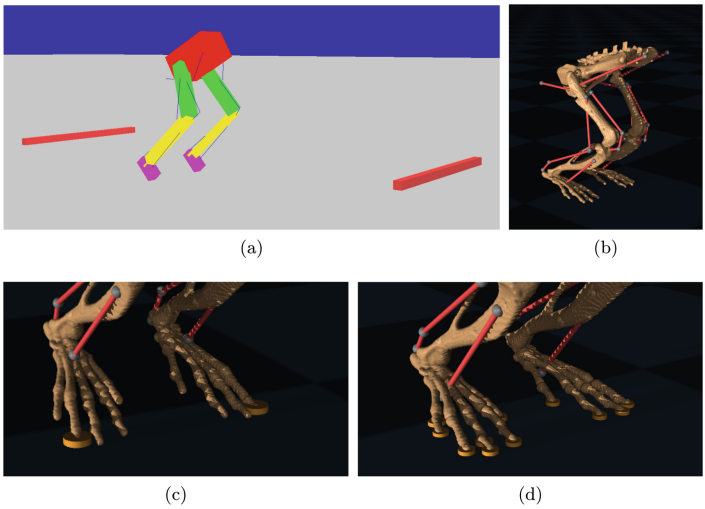

Fig. 1. Biomechanical models of rat hindlimbs. (a) Model in Animatlab2 with additional bodies to prevent falling [14]. (b) Complete model in Mujoco used for this work [23]. (c) Model with rigid toes. (d) Model with passively compliant toes. The orange pucks in (c) and (d) represent the contact points with the ground. (Color figure online)

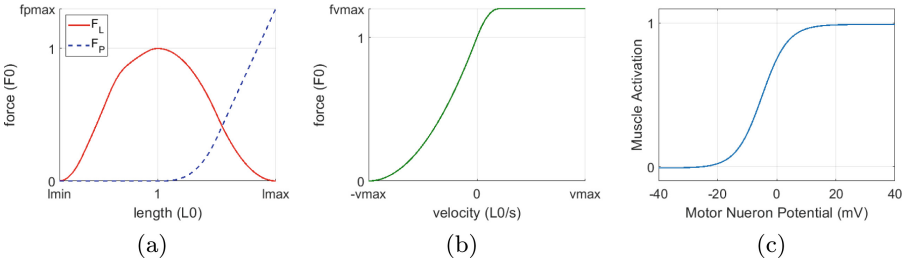

Fig. 2. Muscle model force generation curves. (a) Force-Length and Passive Force curves. *lmin* and *lmax* are computed in the model compiler. (b) Force-Velocity curve. *vmax* is computed in the model compiler [34]. (c) Sigmoidal Curve converting motor neuron activity to muscle activation.

where F_L is the active force as a function of length, F_v is the active force as a function of velocity, L is the length of the muscle, v is the velocity of the muscle, F_0 is the peak active force, F_P is the passive force, and A is a function which converts the potential of the motor neuron, V_{MN}, to a muscle activation between zero and one. Examples of these functions are shown in Fig. 2 [34].

Neural Model. Our objective was to develop a neural model for controlling a biomechanical system. We start by creating a sequence generator which demonstrates continuous cyclic neural activity, inspired by the BSG model proposed by Lindén et al. [24]. A principle component analysis of the BSG showed that the principle components exhibit a limit cycle. While the BSG model relied on random connectivity, our approach aims to design a network that maintains continuous neural activity akin to a BSG but with specific latent dynamics resembling a limit cycle. Notably, the minimum dimensionality of a system to generate oscillations is a 2-dimensional system, we can examine the behavior of a rank two system with the covariance [5]:

$$\sigma = \begin{bmatrix} \sigma_1 & -\sigma_2 \\ \sigma_2 & \sigma_1 \end{bmatrix}. \tag{2}$$

It has been shown that a rank two network with a covariance matrix containing complex eigenvalues indicates an oscillatory behavior [32]. We can apply these principles in designing the connection matrix of a pool of neurons, as was done for RNNs in Beiran et al. Here, we can define a rank two connection matrix, J [5]:

$$J_{ij} = \frac{1}{N} \sum_{r=1}^{2} m_i^{(r)} n_j^{(r)} \tag{3}$$

where N is the number of neurons in the network, $m^{(r)}$ and $n^{(r)}$ are the left and right singular vectors respectfully, and $m^{(r)}$ are also the principle components of the system. The singular vectors are sampled from a single Gaussian distribution with a zero mean and a covariance matrix based upon Eq. 2, $v \sim \mathcal{N}(0, \sigma_{Tot})$ where v are the singular vectors and σ_{Tot} is the covariance matrix [5]:

$$\sigma_{Tot} = \begin{bmatrix} 1 & 0 & \sigma_1 & \sigma_2 \\ 0 & 1 & -\sigma_2 & \sigma_1 \\ \sigma_1 & -\sigma_2 & c & 0 \\ \sigma_2 & \sigma_1 & 0 & c \end{bmatrix}. \tag{4}$$

In this work, we specified the values for the covariance matrix as: $\sigma_1 = 2.25$, $\sigma_2 = 0.25$, and $c = 5.45$.

The resulting connection matrix, J, defines weight based connections. The neural model used in this work, as defined in the Python package SNS-Toolbox [28], is the non-spiking leaky integrator model,

$$C_m \frac{dU}{dt} = -G_m U + I_{app} + \sum_{i=1}^{n} I_{syn_i} \tag{5}$$

where C_m is the membrane capacitance, U is the membrane potential offset by the resting potential ($U = V - E_R$), G_m is the membrane conductance, I_{app} is an applied external current, and I_{syn} is the synaptic current. The synaptic current uses a conductance based model:

$$I_{syn_i} = g_{max_i} \cdot \min\left(\max\left(\frac{U_{pre}}{R}, 0\right), 1\right) \cdot (\Delta E_{syn_i} - U(t)) \tag{6}$$

where g_{max} is the maximum synaptic conductance, U_{pre} is the membrane potential of the pre-synaptic neuron, R is the range of synaptic activity, and ΔE_{syn_i} is the synaptic reversal potential offset by the neural resting potential ($\Delta E_{syn_i} = E_{syn} - E_R$) and describes the function of the synapse. When $\Delta E_{syn_i} < 0$, it indicates an inhibitory synapse. When $\Delta E_{syn_i} > 0$, it indicates an excitatory synapse. The connectivity matrix described in Eq. 3 defines the synapses in terms of weights. To convert this to a conductance based synapse, we define the reversal potentials and maximum synaptic conductance's according to Szczecinski et al. [33].

$$\Delta E_{syn} = \begin{cases} E_{inhibit} & \text{if } J < 0, \\ E_{excite} & \text{if } J \geq 0. \end{cases} \tag{7}$$

$$g_{max} = \frac{JR}{\Delta E_{syn} - JR} \tag{8}$$

The sequence generator is composed of 200 neurons, similar to that of the BSG network proposed by Linden et al. [24]. The activity in the sequence generator defined using Eqs. 2–8 results in continuous neural behavior with the principle components exhibiting a limit cycle, as shown in Fig. 3.

The sequence generator network is then connected to an output level motor circuit consisting of Ia inhibitory neurons, motor neurons, Renshaw cells, and Ia and Ib interneurons to incorporate feedback. Muscle velocity and tension feedback (Ia and Ib, respectfully) are included in the motor circuit. This motor circuit is present in numerous other neural models of locomotive circuitry, typically with an input from pattern generator networks [14,21,26,29]. As the focus of this work is the effectiveness of the sequence generator, the parameters used in the motor circuit model were derived from Deng et al. (2019). Unlike the

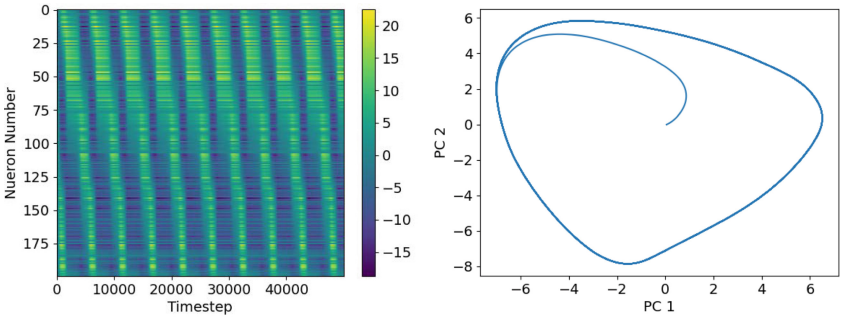

Fig. 3. Sequence Generator Activity. (a) Neuron activity where the color indicates the neuron membrane potential, U, in mV. The x-axis shows the iteration or timestep in the simulation where $dt = 0.1$ ms. (b) Component space showing the rotational behavior of the first two principle components. The principle components are unitless. (Color figure online)

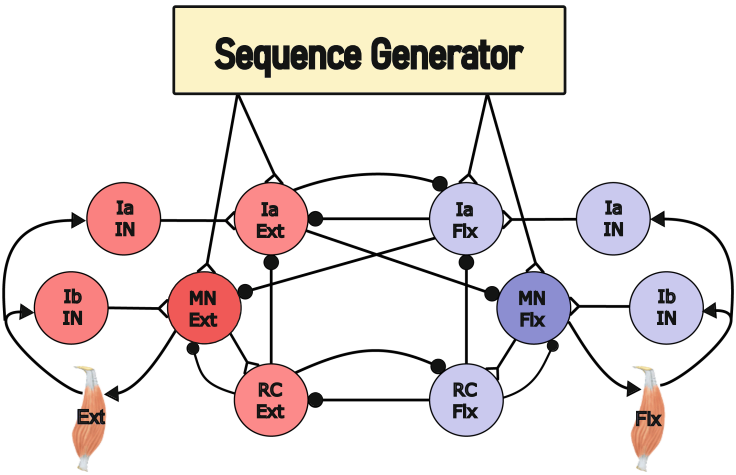

Fig. 4. Motor Circuit receiving input from the sequence generator. The hip, knee, and ankle have separate motor circuits but share the sequence generator. The motor circuit consists of motor neurons (MN), Renshaw cells (RC), Ia and Ib interneurons (IN), and Ia inhibitory neurons. The Ia and Ib interneurons receive velocity and tension feedback, respectively, from the corresponding muscle.

model presented in Deng et al. (2019) type II, length feedback, is not included in the present model. Length feedback was used in previous models as an input to the pattern generator networks [14,29], further analysis of the sequence generator is required to determine how to properly implement length feedback into the network. Figure 4 shows the design of the motor network with input from the sequence generator. Note that the hip, knee, and ankle each have their own motor circuit, but share the sequence generator network.

2.2 Tuning

The tuning process was broken into two stages: the first focusing on how to connect the sequence generator to the motor circuits, and the second focusing on the strength of these connections and the Ia and Ib afferent feedback. In this model, we designate continuous sections of the sequence generator to act as inputs to the flexor and extensor sides of the motor circuits. This stage of tuning dictates the timing of swing and stance in the model. Further tuning of the joint trajectories could be done by tuning the parameters of the motor circuit, however, this has not been done in this work. We first utilized the BFGS nonlinear optimization method, as implemented in SciPy [35] to determine which

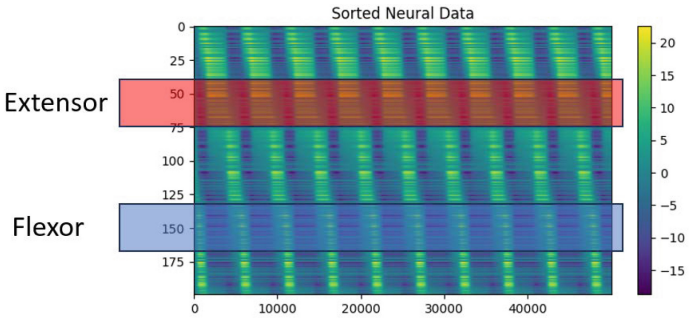

Fig. 5. Designated regions of flexion and extension in the sequence generator. The extensor region (red) and flexor region (blue) are connected to the corresponding sections of the motor circuit. (Color figure online)

regions of the sequence generator to treat as inputs to the flexor and extensor sides of the motor circuits. Examples of these flexor and extensor regions can be seen in Fig. 5. The resulting simulated data of the joint trajectories was compared to animal data of a rat walking on a treadmill, previously collected by Allesandro et al., using a mean square error for single gait trajectories as the loss function. Note that the animal data represents averages over multiple steps, ensuring that the features observed are not artifacts of a single step [2]. The strengths of the synapses from the sequence generator to the motor circuits were fixed during this initial stage in the tuning process and later hand tuned along with the strengths of the Ia and Ib feedback in order to improve and shape the trajectories once the connectivity from the sequence generator was determined.

3 Results

The neural activity shown in Fig. 3 demonstrates the effectiveness of this network design method to produce the rhythmic activity consistent with activity in the spinal cord during locomotive behavior in rats [6]. Integrating these signals with motor circuits consistent with two-layer pattern generator networks [14,29], we are able to control a simplified model of rat hindlimbs with antagonistic muscle pairs controlling the hip, knee, and ankle joints in the sagittal plane. Neurons 50–98 in the sequence generator were identified as the inputs to the extensor neurons of the motor circuits, while neurons 190–198 were identified as the inputs to the flexor neurons of the motor circuits. The number of the neuron corresponds to the order that it is active in the cycle (see Figs. 3 and 5 for examples). Figure 6

Table 1. Connection strengths from the Sequence Generator (SG) to motor circuits.

Synaptic Connection		Maximum Synaptic Conductance (μS)
Hip Motor Circuit	SG to MN Ext	0.03
	SG to MN Flx	0.1
	SG to Ia Ext	0.025
	SG to Ia Flx	1.5
Knee Motor Circuit	SG to MN Ext	0.3515
	SG to MN Flx	0.5
	SG to Ia Ext	0.09
	SG to Ia Flx	1.0
Ankle Motor Circuit	SG to MN Ext	0.2215
	SG to MN Flx	1.5
	SG to Ia Ext	0.15
	SG to Ia Flx	0.16

shows the joint trajectories generated by the neural and biomechanical models in the simulation, showing similar features between the simulated and animal joint trajectories [2]. Table 1 shows the final strengths of the connections from the sequence generator network to the motor circuits.

4 Discussion

This work has demonstrated the effectiveness of a network designed to produce a continuous cycle of neural activity in controlling a biomechanical model of a pair of rat hindlimbs. While there are noticeable differences in the trajectory for a single gait (see Fig. 6) we are still able to identify key components. Among these components noted in both the animal data and the simulation are: in the hip, we see a slight bump with a change in velocity in early extension; in the knee, leveling off in extension with a distinct peak just prior to flexion; and in the ankle, a dip is observed in the middle of extension, just after touch down.

The joint trajectories could likely be improved through further tuning of the motor network. It has been shown that given a reliable oscillator, the limit cycle can be reshaped with a mapping function [1]. Treating the motor circuit as a mapping function to the muscle activation, this network could be tuned to reshape the input from the sequence generator to better control muscle activation during locomotion. The neural model presented in this work also does not incorporate type II muscle feedback. In other works, which used more traditional half-center oscillators, the type II feedback was used as feedback to the pattern generator networks, helping to control the timing of the transition from flexion

to extension and vice versa [14,29]. As the sequence generator presented in this work is constructed as a pool of neurons, it is unclear how to integrate this feedback to achieve a similar impact. Through further analysis of the BSG, Lindén et al. discovered that specific neurons in the network had a more significant impact on the frequency and amplitude of the limit cycle than others. Based on the similar dynamics, it is likely that our network has similar properties, and these neurons would be ideal in integrating the type II feedback. However, further analysis of the sequence generator presented in this work is needed to find such neurons and integrate the feedback.

It should also be noted that the simplified biomechanical model using antagonistic muscle pairs may have also contributed to the differences in joint trajectories shown in Fig. 6. While this simplification is sufficiently able to produce locomotive behavior, it is vastly different than muscle control and coordination of all 38 muscles in the rat hindlimb [36]. We hypothesize that for controlling the more complex model, instead of assigning specific regions for flexion and extension in the sequence generator (see Fig. 5), we can designate small windows of neurons in the sequence generator to connect to motor neurons controlling these muscles, aligning the activity of the sequence generator with muscle activity for each individual muscle. Controlling biomechanical models with these complex muscle synergies is difficult with the half-center model, as not all of the muscles can be classified as flexors or extensors and may be active during both phases. Some half-center models have countered this argument by including additional pattern generators, using the combination of signals to control muscle synergies [13]. However, these additional half-centers add to the complexity of the neural model, leading to the need for further tuning and a more computationally expensive model. To expand the sequence generator model described in

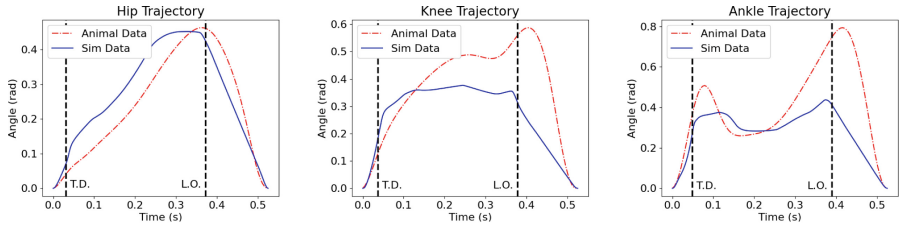

Fig. 6. Joint trajectories for animal and simulated data. The axes were shifted such that both lines start at zero. (a) Hip Joint Trajectory. (b) Knee Joint Trajectory. (c) Ankle Joint Trajectory. T.D. and L.O. indicate touch down and lift off, respectfully, for the simulated data.

this work to more complex muscle synergies, some additional tuning would be required to connect to the additional motor circuits. However, this tuning would be restricted to these lower level circuits, as opposed to the half-center models which require additional tuning to both the lower level circuits and to the additional half-centers involved in driving the rhythmic activity. Future works will expand the biomechanical model to include the full array of muscles in the hindlimb.

5 Conclusion

This study introduces a method of designing a network to model the rhythmic activity in the spinal cord and demonstrates its ability to control a biomechanical model of rat hindlimbs. Through integration with a biomechanical simulation, our neural model successfully controlled antagonistic muscle pairs, resulting in joint trajectories that exhibit similarities to those observed in rats during locomotion. Future work will focus on developing more biologically accurate models and improving joint trajectories. This can be achieved by fine-tuning the motor network and incorporating type II muscle feedback into the sequence generator. Additionally, expanding our biomechanical model to include the full array of muscles in the hindlimb would provide a more comprehensive understanding of how to control muscle synergies during locomotion. It is also important to understand how this model behaves compared to other neural models, future work will explore a comparison of this neural controller to others in the field.

References

1. Ajallooeian, M., Van Den Kieboom, J., Mukovskiy, A., Giese, M.A., Ijspeert, A.J.: A general family of morphed nonlinear phase oscillators with arbitrary limit cycle shape **263**, 41–56 (2013). https://doi.org/10.1016/j.physd.2013.07.016
2. Alessandro, C., Rellinger, B.A., Barroso, F.O., Tresch, M.C.: Adaptation after vastus lateralis denervation in rats demonstrates neural regulation of joint stresses and strains **7**, e38215 (2018). https://doi.org/10.7554/eLife.38215
3. Alexander, R.M.: Three uses for springs in legged locomotion **9**(2), 53–61. https://doi.org/10.1177/027836499000900205
4. Beer, R.D., Quinn, R.D., Chiel, H.J., Ritzmann, R.E.: Biologically inspired approaches to robotics: what can we learn from insects? **40**(3), 30–38 (1997). https://doi.org/10.1145/245108.245118
5. Beiran, M., Dubreuil, A., Valente, A., Mastrogiuseppe, F., Ostojic, S.: Shaping dynamics with multiple populations in low-rank recurrent networks **33**(6), 1572–1615 (2021). https://doi.org/10.1162/neco_a_01381

6. Berg, R., Komi, S., Dmytriyeva, O., Houser, G., Bonfils, M., Kaur, J.: Pedunculopontine-stimulation obstructs hippocampal theta rhythm and halts movement (2024). https://doi.org/10.21203/rs.3.rs-3876253/v1
7. Brown, T.G.: On the nature of the fundamental activity of the nervous centres; together with an analysis of the conditioning of rhythmic activity in progression, and a theory of the evolution of function in the nervous system **48**(1), 18–46 (1914). https://doi.org/10.1113/jphysiol.1914.sp001646
8. Catalano, M.G., Pollayil, M.J., Grioli, G., Valsecchi, G., Kolvenbach, H., Hutter, M., Bicchi, A., Garabini, M.: Adaptive feet for quadrupedal walkers **38**(1), 302–316 (2022). https://doi.org/10.1109/TRO.2021.3088060
9. Chevallier, S., Jan Ijspeert, A., Ryczko, D., Nagy, F., Cabelguen, J.M.: Organisation of the spinal central pattern generators for locomotion in the salamander: biology and modelling **57**(1), 147–161 (2008). https://doi.org/10.1016/j.brainresrev.2007.07.006
10. Chiel, H.J., Beer, R.D.: The brain has a body: adaptive behavior emerges from interactions of nervous system, body and environment **20**(12), 553–557. https://doi.org/10.1016/S0166-2236(97)01149-1
11. Cofer, D., Cymbalyuk, G., Reid, J., Zhu, Y., Heitler, W.J., Edwards, D.H.: AnimatLab: a 3d graphics environment for neuromechanical simulations **187**(2), 280–288 (2010). https://doi.org/10.1016/j.jneumeth.2010.01.005
12. Delp, S.L., Anderson, F.C., Arnold, A.S., Loan, P., Habib, A., John, C.T., Guendelman, E., Thelen, D.G.: OpenSim: open-source software to create and analyze dynamic simulations of movement **54**(11), 1940–1950. https://doi.org/10.1109/TBME.2007.901024
13. Deng, K., Hunt, A.J., Chiel, H.J., Quinn, R.D.: Biarticular muscles improve the stability of a neuromechanical model of the rat hindlimb. In: Meder, F., Hunt, A., Margheri, L., Mura, A., Mazzolai, B. (eds.) Biomimetic and Biohybrid Systems, pp. 20–37. Springer Nature Switzerland (2023). https://doi.org/10.1007/978-3-031-39504-8_2
14. Deng, K., Szczecinski, N.S., Arnold, D., Andrada, E., Fischer, M.S., Quinn, R.D., Hunt, A.J.: Neuromechanical model of rat hindlimb walking with two-layer CPGs **4**(1), 21 (2019). https://doi.org/10.3390/biomimetics4010021
15. Deng, K., Szczecinski, N.S., Hunt, A.J., Chiel, H.J., Quinn, R.D.: Kinematic and kinetic analysis of a biomechanical model of rat hind limb with biarticular muscles. In: Vouloutsi, V., Mura, A., Tauber, F., Speck, T., Prescott, T.J., Verschure, P.F.M.J. (eds.) Biomimetic and Biohybrid Systems, vol. 12413, pp. 55–67. Springer International Publishing (2020). https://doi.org/10.1007/978-3-030-64313-3_7
16. Grillner, S., Zangger, P.: Locomotor movements generated by deafferented spinal-cord. In: Acta Physiologica Scandinavica, vol. 91, pp. A38–A39. Blackwell Science Ltd PO BOX 88, Osney Mead, Oxford, Oxon, England OX2 0NE (1974)
17. Grillner, S., Zangger, P.: On the central generation of locomotion in the low spinal cat **34**(2) (1979). https://doi.org/10.1007/BF00235671
18. Grillner, S.: Biological pattern generation: the cellular and computational logic of networks in motion **52**(5), 751–766 (2006). https://doi.org/10.1016/j.neuron.2006.11.008

19. Guertin, P.A.: The mammalian central pattern generator for locomotion **62**(1), 45–56 (2009). https://doi.org/10.1016/j.brainresrev.2009.08.002
20. Hill, A.V.: The heat of shortening and the dynamic constants of muscle **126**(843), 136–195 (1938). https://doi.org/10.1098/rspb.1938.0050
21. Ivashko, D., Prilutsky, B., Markin, S., Chapin, J., Rybak, I.: Modeling the spinal cord neural circuitry controlling cat hindlimb movement during locomotion **52–54**, 621–629 (2003). https://doi.org/10.1016/S0925-2312(02)00832-9
22. Jackson, C., Chardon, M., Wang, Y.C., Rudi, J., Tresch, M., Heckman, C.J., Quinn, R.D.: Multimodal parameter inference for a canonical motor microcircuit controlling rat hindlimb motion. In: Meder, F., Hunt, A., Margheri, L., Mura, A., Mazzolai, B. (eds.) Biomimetic and Biohybrid Systems, vol. 14158, pp. 38–51. Springer Nature Switzerland (2023). https://doi.org/10.1007/978-3-031-39504-8_3
23. Johnson, W.L., Jindrich, D.L., Roy, R.R., Reggie Edgerton, V.: A three-dimensional model of the rat hindlimb: musculoskeletal geometry and muscle moment arms **41**(3), 610–619. https://doi.org/10.1016/j.jbiomech.2007.10.004
24. Lindén, H., Petersen, P.C., Vestergaard, M., Berg, R.W.: Movement is governed by rotational neural dynamics in spinal motor networks **610**(7932), 526–531 (2022). https://doi.org/10.1038/s41586-022-05293-w
25. Massarelli, N., Yau, A., Hoffman, K., Kiemel, T., Tytell, E.: Understanding locomotor rhythm in the lamprey central pattern generator. In: Letzter, G., et al. (eds.) Advances in the Mathematical Sciences, vol. 6, pp. 157–172. Springer International Publishing (2016). https://doi.org/10.1007/978-3-319-34139-2_6
26. McCrea, D.A., Rybak, I.A.: Organization of mammalian locomotor rhythm and pattern generation **57**(1), 134–146 (2008). https://doi.org/10.1016/j.brainresrev.2007.08.006
27. Melo, K., Horvat, T., Ijspeert, A.J.: Minimalist design of a 3-axis passive compliant foot for sprawling posture robots. In: 2019 2nd IEEE International Conference on Soft Robotics (RoboSoft), pp. 788–794. IEEE (2019). https://doi.org/10.1109/ROBOSOFT.2019.8722792
28. Nourse, W.R.P., Jackson, C., Szczecinski, N.S., Quinn, R.D.: SNS-toolbox: an open source tool for designing synthetic nervous systems and interfacing them with cyber-physical systems **8**(2), 247 (2023). https://doi.org/10.3390/biomimetics8020247
29. Rybak, I.A., Stecina, K., Shevtsova, N.A., McCrea, D.A.: Modelling spinal circuitry involved in locomotor pattern generation: insights from the effects of afferent stimulation **577**(2), 641–658 (2006). https://doi.org/10.1113/jphysiol.2006.118711
30. Selverston, A.: The stomatogastric ganglion. In: Reference Module in Neuroscience and Biobehavioral Psychology, p. B9780128093245211668. Elsevier (2017). https://doi.org/10.1016/B978-0-12-809324-5.21166-8
31. Seth, A., et al.: OpenSim: Simulating musculoskeletal dynamics and neuromuscular control to study human and animal movement **14**(7), e1006223. https://doi.org/10.1371/journal.pcbi.1006223
32. Strogatz, S.H.: Nonlinear dynamics and chaos: with applications to physics, biology, chemistry, and engineering, pp. 198–212. Westview Press, a member of the Perseus Books Group, second edition edn. (2015), OCLC: ocn842877119
33. Szczecinski, N.S., Hunt, A.J., Quinn, R.D.: A functional subnetwork approach to designing synthetic nervous systems that control legged robot locomotion **11**, 37 (2017). https://doi.org/10.3389/fnbot.2017.00037

34. Todorov, E., Erez, T., Tassa, Y.: Mujoco: A physics engine for model-based control. In: 2012 IEEE/RSJ International Conference on Intelligent Robots and Systems, pp. 5026–5033. IEEE (2012). https://doi.org/10.1109/IROS.2012.6386109
35. Virtanen, P., et al.: SciPy 1.0: fundamental algorithms for scientific computing in python **17**(3), 261–272 (2020). https://doi.org/10.1038/s41592-019-0686-2
36. Young, F., Rode, C., Hunt, A., Quinn, R.: Analyzing moment arm profiles in a full-muscle rat hindlimb model **4**(1), 10 (2019). https://doi.org/10.3390/biomimetics4010010